Nonlinear MHD in the DAG Confinement Configuration

H.R. Strauss
New York University, New York, New York
D. Weil
Hebrew University, Jerusalem, Israel

Abstract. The DAG magnetic fusion confinement configuration is a spheromak - like toroidal device. It consists of central vertical current channel, and an outer toroidal chamber with a toroidal current. It has a special magnetic topology. Unlike most toroidal magnetic confinement configurations, which have a magnetic field with homotopic invariant of zero, it has a magnetic field with homotopic invariant of unity. Whether this has consequences for plasma confinement is a motive for this study. A restricted class of computations done so far, using the M3D code, indicate stability for $\beta < 15\%$. For higher β, the simulations exhibit turbulent magnetic behavior similar to spheromaks and reverse field pinches.

I. Introduction

The DAG [1] magnetic fusion confinement configuration is a spheromak - like toroidal device. It consists of central vertical current channel, and an outer toroidal chamber with a toroidal current. It has a special magnetic topology. Unlike most toroidal magnetic confinement configurations, which have a magnetic field with homotopic invariant of zero, it has a magnetic field with homotopic invariant of unity [2]. Whether this has consequences for plasma confinement is a motive for this study. A restricted class of computations done so far, using the M3D code, indicate ideal and resistive MHD stability for $\beta < 15\%$. For higher β, the simulations exhibit turbulent magnetic behavior similar to spheromaks and reverse field pinches.

The M3D (Multi-level 3D) project [3, 4] carries out simulation studies of plasmas using multiple levels of physics, geometry, and grid models. The present study is done with a resistive MHD model. M3D combines a two dimensional unstructured mesh with finite element discretization in poloidal planes [5], with a pseudo spectral representation in the toroidal direction. The unstructured mesh used in the calculations is shown in Fig.1(a). A difference from the original DAG is presence of a small central hole, which is required by the present version of M3D. A top view of the mesh, showing the small central hole, is in Fig.1(b).

II. Equilibrium

The DAG configuration is obtained as a relaxed Taylor[6] state. Like the spheromak or RFP, it is a solution of the force free condition

$$\mathbf{J} = \alpha \mathbf{B} \tag{1}$$

With an equilibrium magnetic field of the usual form

$$\mathbf{B} = \nabla\psi \times \nabla\phi + I\nabla\phi \tag{2}$$

then ψ satisfies

$$\frac{\partial^2\psi}{\partial R^2} - \frac{1}{R}\frac{\partial\psi}{\partial R} + \frac{\partial^2\psi}{\partial Z^2} = -\alpha^2\psi \tag{3}$$

and

$$I = \alpha\psi \tag{4}$$

A special solution has the form [1]

$$\psi = \sum_{k=0} \frac{a_k R}{(\mu^2 - k^2)^{1/2}} J_1[R(\mu^2 - k^2)^{1/2}] \cos(kZ) \tag{5}$$

A DAG configuration has one elliptic and one hyperbolic axis, with toroidal magnetic field in opposite directions at the axes. Combinations of $k = 0$ and other k terms in the sum have this property, as well as having closed flux surfaces. The following example has $\mu = 25$, $k = 23$, and $a_{23} = -0.4a_0$. The poloidal and toroidal fluxes are shown in Fig.2. The lengths have been rescaled.

The force free equilibria have zero pressure. Pressure is added in the form

$$p = p_0\psi^2 \tag{6}$$

and the resulting state evolved in time. With viscous dissipation, a finite pressure equilibrium is found, similar to the zero pressure equilibrium.

The finite pressure initial states equilibrate on a rapid time scale. The pressure expands radially until force balance is reached. The current, and to a lesser extent, the toroidal magnetic field, also adjust. The pressure is broadens, and there is some current at the x point, indicating magnetic reconnection and some loss of poloidal magnetic flux.

III. Long Time Stable Evolution

The equilibrium is allowed to evolve, for hundreds of Alfvén times. The evolution occurs in three dimensions, so that instabilities can occur. A small three dimensional perturbation is added, from which unstable modes could grow. The resolution in the toroidal direction permits toroidal modes of the form $\exp in\phi$ with $n \leq 6$. This is adequate to test for long wavelength instabilities with $nq \sim 1$, of the sort that occur in RFPs[7] and spheromaks[8]. Short wavelength interchange modes require much higher resolution. The existence of short wavelength modes is questionable because of finite Larmor radius stabilization[9]. The low pressure equilibrium shown here appears stable to fast growing modes. In this case $\beta = 0.11$, where $\beta = 2 < p > / < B^2 >$, the ratio of volume averaged plasma pressure to volume averaged magnetic pressure.

In the evolution, sources of toroidal current and pressure are included, to oppose dissipative diffusion. The ratio of resistive diffusion time to Alfvén time, in all the computations, is $S = 10^3$. The poloidal and toroidal flux at $t = 328t_A$ is shown in Fig.2, where $t_A = R/v_A$ is the Alfvén time, where R is the major radius, and v_A s the Alfvén speed.

The current and pressure at the same time are shown in Fig.3. They are close to their initial states.

The toroidal magnetic field, along the midplane, and the q profile, are shown in Fig.4. The toroidal magnetic field reverses near the magnetic x point, giving a homotopic invariant of unity[2]. The q profile shows that instabilities with toroidal mode number $n = 1$ cannot be resonant, because $q < 1$ everywhere. The $n = 1$ mode has been problematic for spheromak experiments[8]. There might be resonances at the separatrix with $n = -1$, but these instabilities would have to be highly localized, and in fact are not seen in the simulations.

IV. Unstable Evolution

In the case of higher $\beta = 0.22$, the configuration is unstable. The initial state is formed as before, increasing the pressure source and allowing the configuration to relax to equilibrium on a short time scale. The main difference from the low β case is the current and pressure, shown in Fig.5. The current is strongly peaked toward the large R side. The pressure is also somewhat shifted to large R. This effect is well known in tokamaks. The other variables are similar to the low β case.

The current and pressure at $t = 123t_A$ are shown in Fig.6. The current and pressure are highly distorted by three dimensional instabilities. The current and pressure perturbations have a structure typical of resonant kink modes. They saturate at relatively low amplitude by flattening of current and pressure profiles, similar to the relaxation process in RFPs [7].

The instability can be seen in the velocity potential Φ (the electrostatic potential). In Fig.7(a) are contours of Φ in the plane $\phi = 0$, showing long wavelength structure. In Fig.7(b) are contours of Φ in the plane $Z = 0$, showing toroidal Fourier harmonic $n = 4$, which is resonant in that it can satisfy $nq = 1$ for $q = .25$.

Further simulations indicate that the stability boundary of this configuration is about $\beta < 15\%$.

V. DAG - RFP Stable Evolution

The central hole in the simulations suppresses instabilities of the central poloidal current column flowing vertically on open field lines into conductors (at $Z = \pm 0.925$ in the figures). These instabilities are important for a spheromak - like startup. A poloidal current is driven electrostatically between electrodes; the current becomes kink unstable and eventually relaxes into a more or less two dimensional steady state [8]. Future simulations with different central boundary conditions will be required to assess stability of the central current channel.

As an alternative for a possibly less turbulent start up one might inductively drive a toroidal current, using a center hole, similar to an RFP. The vertical central current can be eliminated.

It is a simple modification of the DAG initial state to set the poloidal and toroidal current equal to zero on open field lines. This can then be evolved with nonzero pressure as before. Eliminating current on the open field lines prevents reversal of the toroidal magnetic field, so the topological invariant of the DAG is zero. This does not seem to have a substantial effect on the MHD stability limit, which is similar to the previous cases. A stable example is shown in the following.

The poloidal and toroidal flux at $t = 350 t_A$ is shown in Fig.8. The toroidal current and pressure at the same time are shown in Fig.9. These are all similar to their initial states. The toroidal flux and current remain zero on the open field lines outside the x - point of the poloidal flux. In this case $\beta = 16\%$. The β tends to be somewhat higher in this configuration, because it has somewhat lower total magnetic energy.

The toroidal magnetic field, along the midplane, and the q profile, are shown in Fig.10. Because the toroidal magnetic field does not reverse sign, q also does not reverse sign. The spike in q indicates the separatrix. The height of the spike would increase with higher numerical resolution.

VI. Conclusion

Three dimensional dissipative initial value simulations indicate the stability of low pressure DAG - like configurations. The main difference from the original DAG is the rigid boundary in the center of the computational boundary. For moderate $\beta < 0.15$ the DAG is stable. For higher β it is unstable to internal kink like modes. These modes do not cause disruption, as in a tokamak, but rather produce a turbulent steady state, as in an RFP.

It is possible to have zero current on open field lines, turning the DAG into a more RFP like configuration, which has similar equilibrium and stability to the DAG.

References

[1] WEIL, D. "The Dag Topology: An RFP with Inner Divertor Free of Linking Coil," Comments Plasma Phys. Controlled Fusion, **13**, p 45 - 56 (1989); U.S. patent 5,147,596 (1992).

[2] FINKELSTEIN D. and WEIL, D., "Magnetohydrodynamic Kinks in Astrophysics," Int. J. Theor. Phys. **17**, 201 (1978).

[3] PARK, W., BELOVA, E.V., FU, G.Y., TANG, X.Z., STRAUSS, H.R., SUGIYAMA, L.E., "Plasma Simulation Studies using Multilevel Physics Models" Phys. Plasmas **6** 1796 (1999).

[4] SUGIYAMA, L.E., PARK, W., STRAUSS, H.R., HUDSON, S.R, STUTMAN, D., TANG, X.Z., Studies of Spherical Tori, Stellarators and Anisotropic Pressure with M3D, Nucl. Fusion (2001).

[5] STRAUSS, H.R. and LONGCOPE, W., An Adaptive Finite Element Method for Magnetohydrodynamics, J. Comput. Phys. 147, 318 - 336 (1998).

[6] Taylor, J. B., "Relaxation of toroidal plasma and generation of reverse magnetic fields," PRL 33, 1139 (1974).

[7] Prager, S. C., "Transport and fluctuations in reversed field pinches," Plasma Physics and Contr. Fusion 32, 903 (1990).

[8] HILL, D. N., BULMER, R. H., COHEN B. I., HOOPER, E. B., LODESTRO, L. L., MATTOR, N., et al., Spheromak formation studies in SSPX, Eighteenth IAEA Fusion Energy Conference, Sorrento, Italy, F1-CN77-ICP/09 (2000)

[9] H.R. Strauss, G.Y. Fu, L.E. Sugiyama, W. Park, J. Breslau, Nonlinear MHD and Energetic Particle Modes in Stellarators, Nineteenth IAEA Fusion Energy Conference, Lyon, France, IAEA-CN-94/TH/P2-12 (2002).

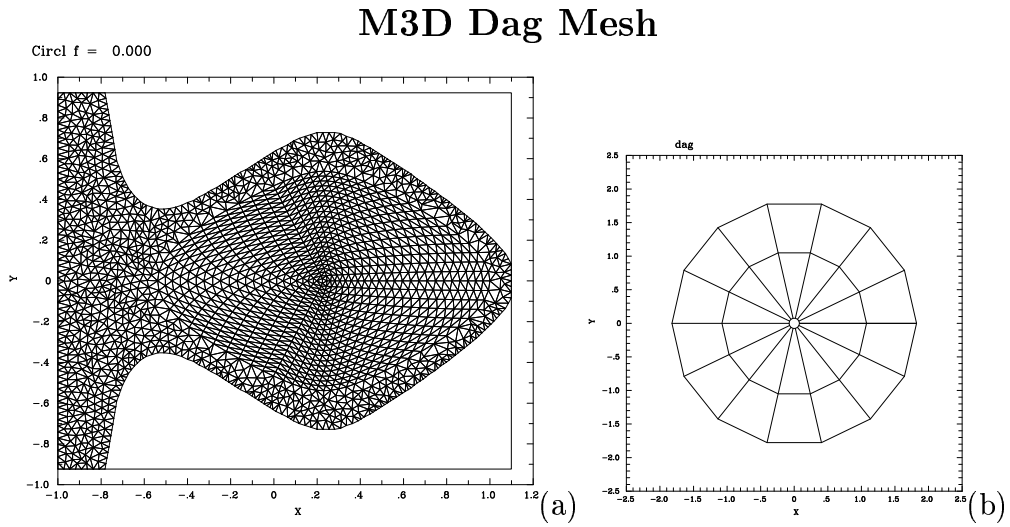

Figure 1: Mesh (a) poloidal plane (b) top view of toroidal mesh

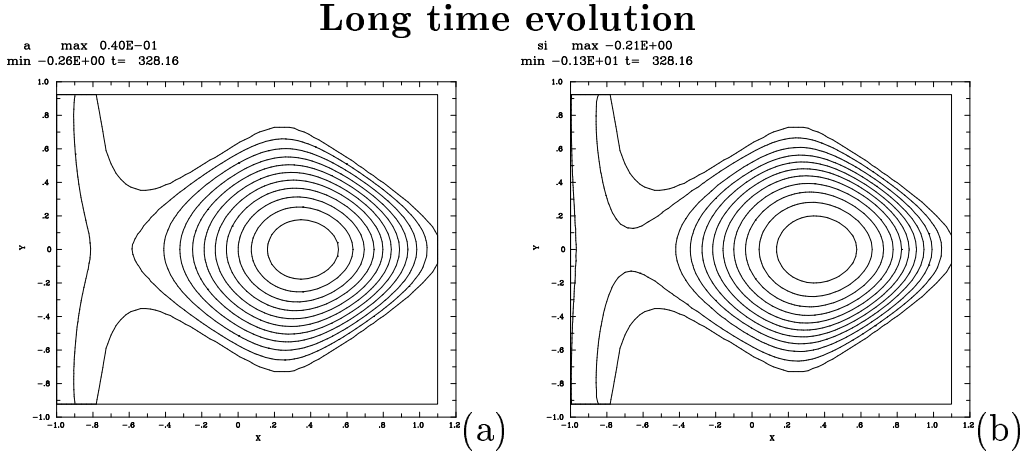

Figure 2: (a) Poloidal Flux (b) Toroidal Flux at t = $328t_A$

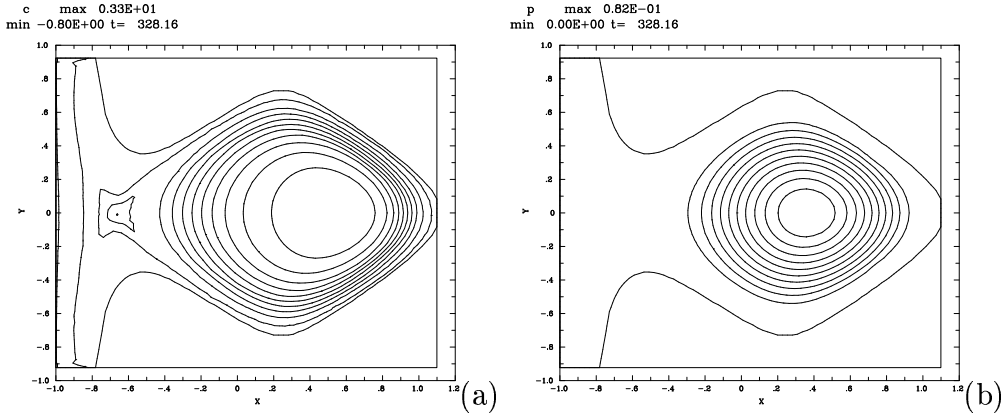

Figure 3: (a) Toroidal current (b) Pressure at $t = 328t_A$

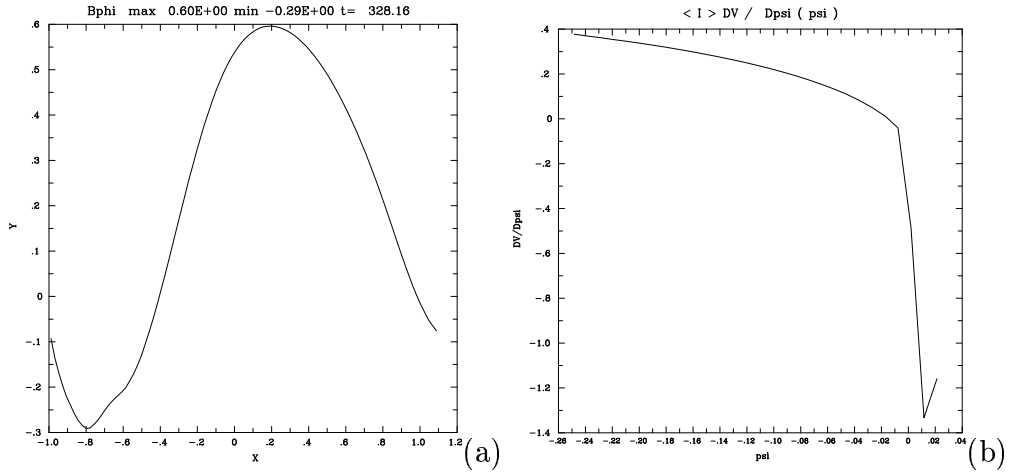

Figure 4: (a) B_ϕ (b) q

High β Instability

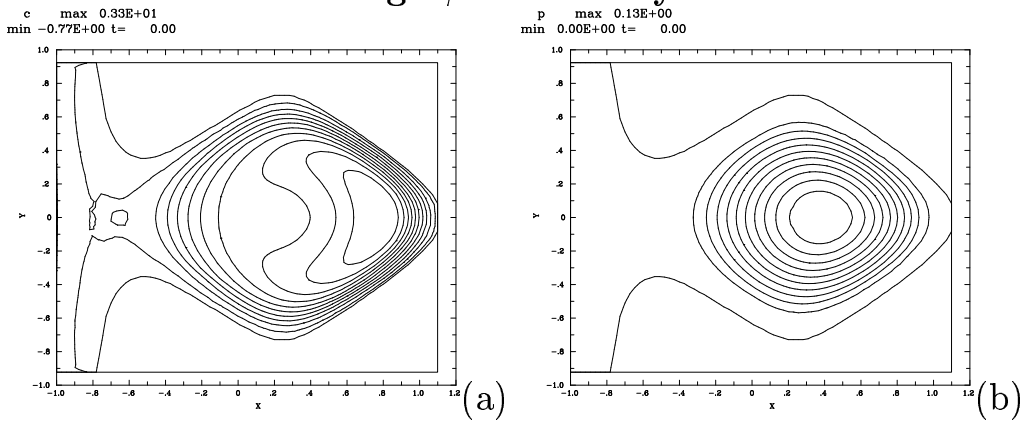

Figure 5: (a) Toroidal current (b) Pressure at $t = 0t_A$

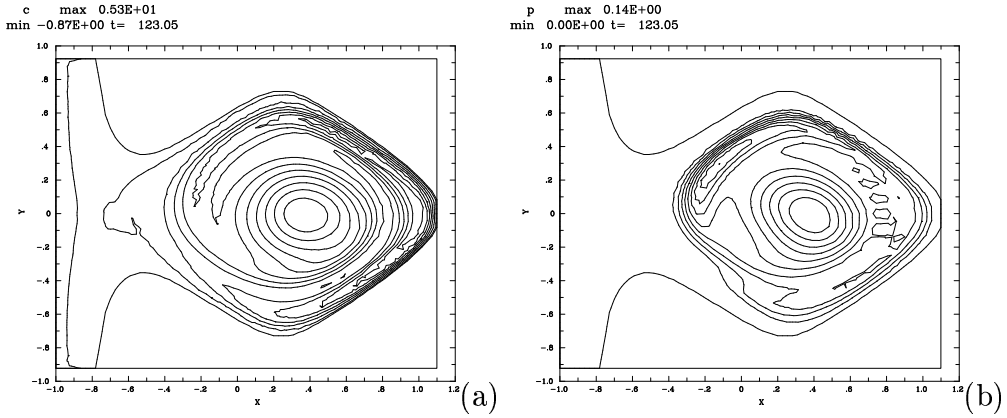

Figure 6: (a) Toroidal current (b) Pressure at $t = 123t_A$

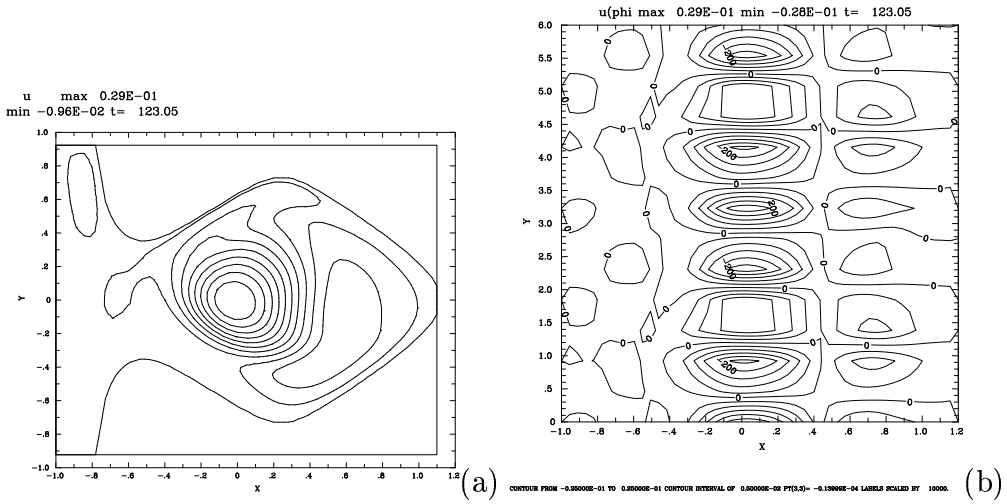

Figure 7: (a) velocity potential Φ at $t = 123t_A$ (b) velocity potential Φ in midplane $Z = 0$.

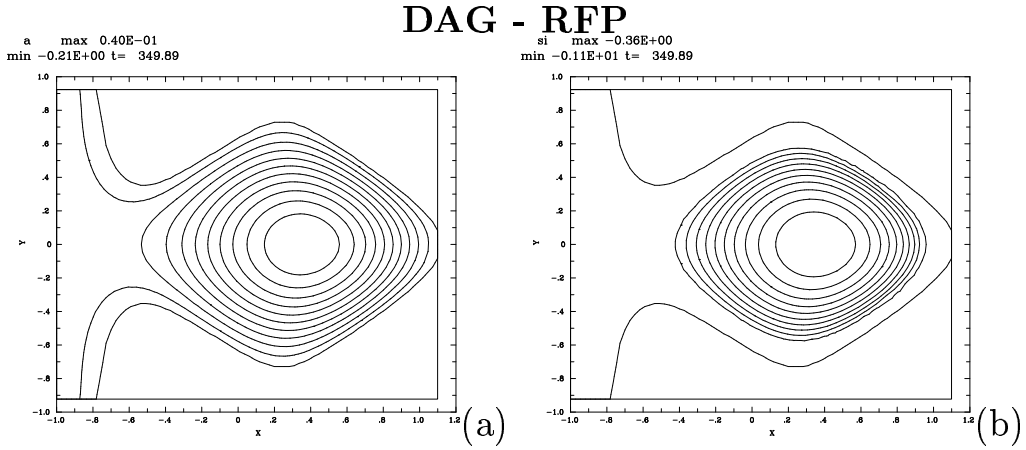

Figure 8: (a) Poloidal Flux (b) Toroidal Flux at t = $350t_A$

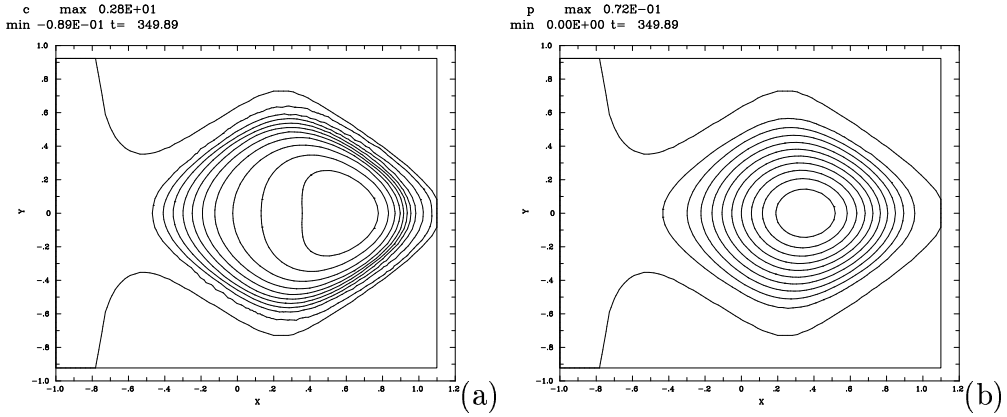

Figure 9: (a) Toroidal current (b) Pressure at $t = 350t_A$

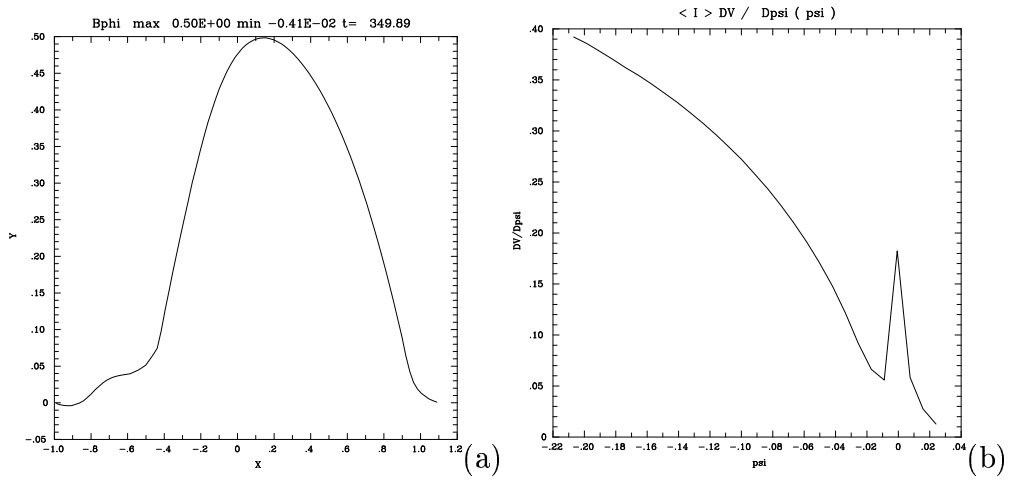

Figure 10: (a) B_ϕ (b) q